ISSN 1392–1320 MATERIALS SCIENCE (MEDŽIAGOTYRA). Vol. 16, No. 4. 2010

Transformation Kinetics of $M_{23}C_6$ Carbide Lattice Parameters in Low Alloyed Steel

Arūnas BALTUŠNIKAS [1, 2 *], Irena LUKOŠIŪTĖ [1], Rimantas LEVINSKAS [1]

[1] *Lithuanian Energy Institute, Breslaujos 3, LT-44403 Kaunas, Lithuania*
[2] *Department of Silicate Technology, Kaunas University of Technology, Radvilenu 19, LT-50254 Kaunas, Lithuania*

Received 02 September 2010; accepted 12 November 2010

Power plant steel 12X1MΦ, taken from the as-installed condition through to 270000 h service-exposed and accelerated aged in laboratory conditions, have been characterized with optical microscopy and X-ray diffraction. Microscopy showed that during heat treatment a number of microstructural changes occurs. Initially formed pearlite disappeared and carbide coarsening also is detectable in steel exploited for long periods and during accelerated ageing. X-ray diffraction revealed that carbide $M_{23}C_6$ crystal lattice parameter changes as a function of service time or heat exposure in laboratory conditions. Johnson-Mehl-Avrami law was adapted to express the dependence of carbide $M_{23}C_6$ crystal lattice parameter changes in a double logarithmic plot. The obtained linear relationship could be applied for steel real state assessment.
Keywords: power plant steel, carbide, optical microscopy, XRD, lattice parameter, kinetics, JMA, life assessment.

1. INTRODUCTION

One of the main directions of power plant operating management is estimating the remaining life of high temperature power generation components. Solution of this problem is very important both for economy and safety reasons but is quite complicated [1, 2].

A various type of techniques has been applied to the study of exploited materials such as mechanical (creep and toughness, fatigue, hardness), ultrasonic, magnetic, electrical and structural testing in order to predict the remnant service life of equipment [3 – 5]. Stress-rupture (SRT) test is widely used in the estimation of creep life of high temperature materials instead of usual creep test because it does not need long periods of time giving good results about the creep behavior of these materials [6]. Widely accepted technique – Larson-Miller parameter (LMP) can be used to extrapolate the results obtained from SRT to the real service conditions [7, 8]. Others equations are usable to adjust short-time mechanical experiments data for prediction of long term behavior of equipment [9].

Despite the fact that the mechanical testing predominates over the other steel state assessment techniques, the estimation of the structure degradation level is very promising because of the potentiality to determine real steel damage reasons [10, 11].

One of the microstructural parameters useful to monitor the structural degradation and suitable for the life assessment is the dependence of the crystallite size of carbides with service life of power plant steel [12].

The evolution of carbides precipitation during accelerated ageing and exploitation of low alloyed heat resistant steel 12X1MΦ was established in our previous work [13]. The obtained carbides transformation sequence may find application for assessment a thermal history of power plant components.

The dependence of the relative amount of Fe_3C and $M_{23}C_6$ carbides in the steel 12X1MΦ on ageing time and temperature have been determined previously using integral intensity of X-ray diffraction peaks (031) for cementite Fe_3C and (422) for $M_{23}C_6$ [14]. These data were applied for modeling transformation of carbides and the prediction remnant life of steel by using the classical Johnson-Mehl-Avrami (JMA) law. However, this methodology is limited to quite a short service time of the 12X1MΦ steel due to the termination of carbide $M_{23}C_6$ peaks integrated intensities changes which achieve a constant value after not long service duration [14].

Otherwise it was shown that the lattice parameter of carbide $M_{23}C_6$ in 12X1MΦ steel continuously increases during steel exploiting time [15]. So, this important finding could be useful for power plant steel 12X1MΦ state assessment and remnant life prediction.

In this work the transformation kinetics of cubic carbide $M_{23}C_6$ lattice parameter a in steel 12X1MΦ accelerated aged in laboratory conditions as well as service-exposed has been investigated. This research may find application to steel state and remnant life assessment.

2. EXPERIMENTAL

The chemical composition of steel 12X1MΦ used in this study is shown in Table 1.

Table 1. Concentrations in wt % of the major alloying elements in 12X1M1Φ steel [16]

Element	C	Cr	Mo	V	Mn	Si
Concentration	0.15	1.20	0.35	0.30	0.70	0.37

Carbide phase of steel was highlighted during the electrochemical etching of the steel samples (size $20 \times 10 \times 10$ mm) in 5 % hydrochloric acid solution thus relatively increasing carbide concentration on the samples surface. Power supply 1621A BK Precision was used for this process. Electrochemical etching of the samples at $(130 – 150)$ mA/cm^2 current densities lasted for 8 – 10 hours. Then carbides powder extracted from the steel were collected on the bottom of the flask, several times washed

*Corresponding author. Tel.: +370-37-401906; fax: +370-37-351271.
E-mail address: *abalt@mail.lei.lt* (A. Baltušnikas)

with warm water and dried during 24 h at 80 °C temperature.

The extracted carbides were dispersed on a nonreflective substrate and X-ray diffraction patterns were obtained with a computer-automated diffractometer DRON-6. Diffraction patterns were recorded at 35 kV and 20 mA. Scanning was carried out at a step size of 0.02° (2θ) and counting time was 5 seconds per step. Flat diffracted beam pyrolitic graphite monochromator was used to separate CuK_α radiation. Equipment was calibrated by corundum α-Al_2O_3 (99.9 %) standard. Silicon powder standard was prepared from silicon single crystal and has been added to analyzed samples of extracted carbide residues for precision lattice parameter measurements. The powder X-ray diffraction patterns of extracted carbides were identified with references available in PDF-2 data base [17] and according to crystallographic features.

The full profile analysis of each diffractogram of carbides extracted from steel 12X1MΦ was carried out by program Powder Cell [18] using a Le Bail pattern decomposition method [19] and accurate crystal lattice parameters of precipitated carbide $M_{23}C_6$ have been calculated (Fig. 1). As starting crystal structure models of identified carbides for Le Bail profiles fitting were used: silicon Si – cubic lattice, space group Fd3m (No. 227), cementite Fe_3C – orthorhombic structure, space group Pnma (No. 62), vanadium carbide VC – cubic lattice, space group Fm-3m (No. 225), $M_{23}C_6$ carbide – cubic lattice, Fm-3m (No. 225) and M_7C_3 carbide – orthorhombic lattice, Pnma (No. 62) [17].

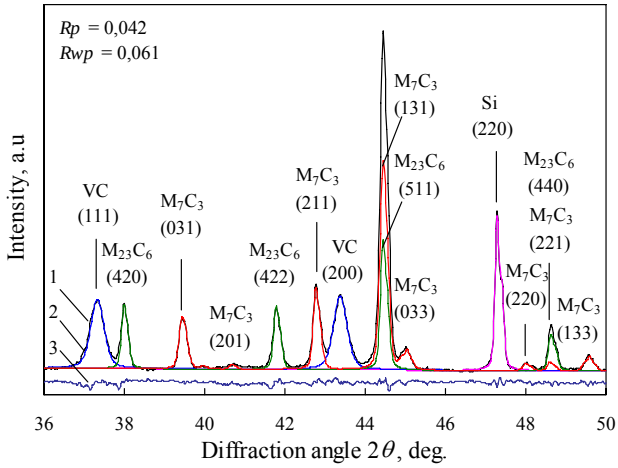

Fig. 1. The example of powder X-ray diffraction pattern of extracted carbides from steel 12X1MΦ after the final Le Bail's fitting: 1 – the observed scattered intensity (Y_i^{obs}); 2 – the calculated intensity (Y_i^{calc}); 3 – the difference between the observed and calculated intensities ($Y_i^{obs} - Y_i^{calc}$)

The transformation kinetics of heat resistant steel carbide $M_{23}C_6$ lattice parameters were visualized using classical John-Mehl-Avrami (JMA) equation for isothermal conditions [20]:

$$x(t) = 1 - \exp\left[-(kt)^n\right], \quad (1)$$

where $x(t)$ is change of lattice parameter a at time t, k is lattice transformation rate constant, t is time, and n is a constant which can be related with different processes.

The linearized form of this equation is [20]:

$$\ln\left[-\ln(1 - x(t))\right] = n\ln k + n\ln t. \quad (2)$$

This equation can be applied to crystallization of amorphous materials, nucleation, growth of new phase kinetics, the analysis of depositions in surface science and etc [21].

Mechanical grinding of the exploited and aged at elevated temperatures steel samples (size 10 × 10 × 5 mm) was done in Buechler Ecomet II device with a polishing fluid Buechler Micropolish II 0.05 μm (γ-Al_2O_3 – water suspension). In order to highlight the steel microstructure, the polished surface was etched 20 s – 25 s by 4 % Nital solution. Microstructure of the samples surface was analyzed by an optical microscope Olympus BX51TF with digital 21 MPix camera QImaging and QCapture software.

3. RESULTS AND DISCUSSION

Changes of microstructure of 12X1MΦ steel surface during its exploitation and ageing were observed using light optical microscopy. Figure 2 shows the optical microscope image of a 5 %-Nital etched-surface.

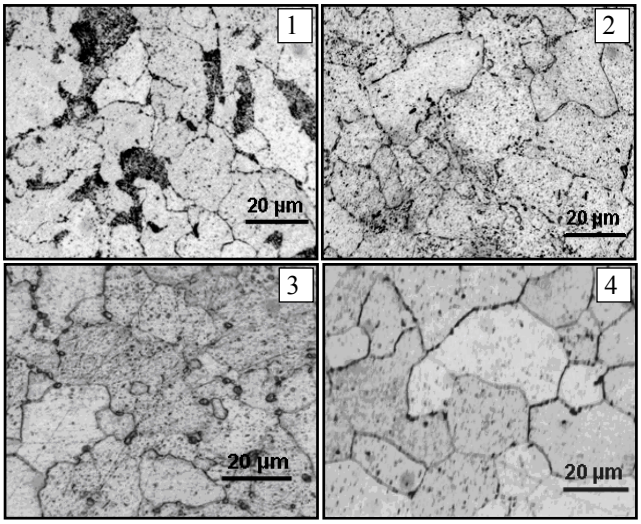

Fig. 2. Optical micrographs of 12X1MΦ steel etched by 4 % Nital solution. Pictures: 1 – virgin; 2 – 151000 h exploited at 550 °C and 14 MPa pressure; 3 – heated at 650 °C during 2400 h; 4 – heated at 700 °C during 744 h

In optical microscopy image of virgin steel (Fig. 2, picture 1) pearlite (which appears as black phases) and ferrite grains are observed, however it is difficult to identify fine carbide compositions. After the ageing at 650 °C and 700 °C during 2400 and 744 hours respectively the density of grain-boundary carbides increased visibly, chains of carbides along the grains of ferrite are formed (Fig. 2, pictures 3 and 4), also coalescence of carbides particles could be seen inside ferrite grains and full destruction of pearlitic structure is detected (Fig. 2, picture 4). In steel exploited 151000 h fine carbide particles in ferrite grains and grain boundaries are observed (Fig. 2, picture 2). After analysis of optical microscopy pictures it was established that the similar microstructural processes during steel exploitation as well as ageing at elevated temperatures in laboratory conditions are generated.

The examples of XRD patterns of carbides extracted from aged and exploited steel 12X1MΦ are presented in Figure 3.

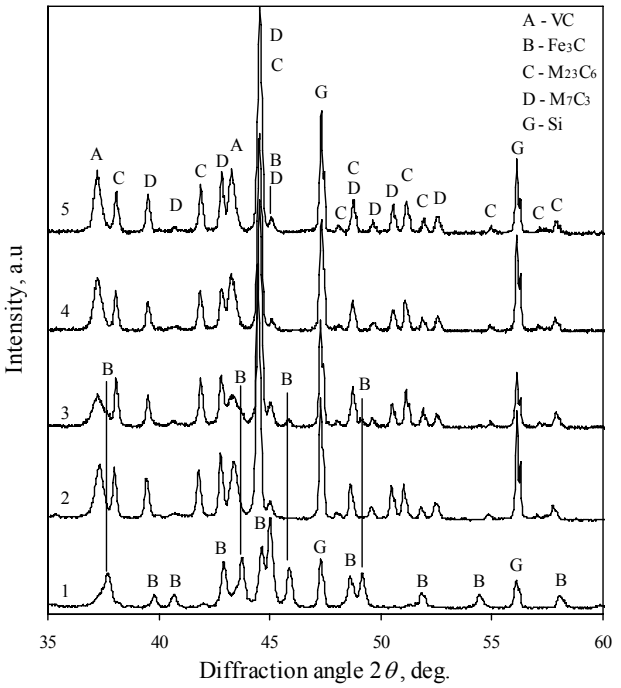

Fig. 3. Selected powder X-ray diffraction patterns of carbides extracted from steel 12X1MΦ. Curves: 1 – virgin; 2 – exploited 227000 h at 550 °C; 3 – heated 3144 h at 600 °C; 4 – 2400 h at 650 °C; 5 – 744 h at 700 °C temperature

Diffractogram 1 in Fig. 3 shows that cementite Fe_3C is present in the virgin steel as a major carbide phase. Only traces of carbides VC, $M_{23}C_6$, M_7C_3 are detectable. Ageing during service and in laboratory conditions caused precipitation of carbides VC, $M_{23}C_6$, M_7C_3 and diminishing of Fe_3C (Fig. 3, curves 2 – 5). Also those diffractograms (Fig. 3, 2 – 5 curves) shows that carbide precipitation evolution is highly comparable, indicating that structural changes during ageing in exploitation (curve 2) as well as in laboratory conditions (curves 3 – 5) are similar too. Thus, structural factor – the carbide $M_{23}C_6$ crystal lattice parameter a value, determined previously as constantly increased during steel exploitation or heating in laboratory conditions [11] – was measured from X-ray diffractograms. Changes of carbide $M_{23}C_6$ crystal lattice parameter a values as a function of steel service and ageing at three temperatures exposure are shown in Fig. 4. It was determined that the experimentally measured parameter a values at all temperatures are increased according to power law (Fig. 4, curves 1 – 4). The carbide $M_{23}C_6$ parameter a value changes from 1.05397 nm in virgin steel to 1.05808 nm in steel exploited during 270000 h.

Those dependences were expressed by Johnson-Mehl-Avrami equation and were drawn in a double logarithmic plot (Fig. 5, curves 1, 3 – 5). Obtained relationships $\ln[-\ln(a_0/a_t)]$ vs. $\ln t$ are linear and proved that JMA low is valid.

Therefore, the linear equations (Fig. 5, curves 3 – 5) give values of carbide $M_{23}C_6$ lattice parameters transformation rate constant k (Table 2), and the transformation mechanism constant $n = 0.4$ for all experimental temperatures have been obtained from the slope of those lines.

Then, the activation energy E_a has been calculated from the equation [22]:

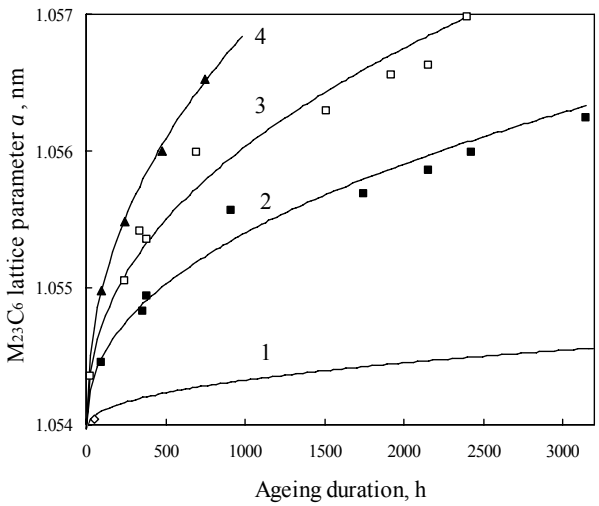

Fig. 4. The changes of lattice parameter a of carbide $M_{23}C_6$ in 12X1MΦ steel depending on ageing time in service conditions – 1, ageing at 2 – 600 °C, 3 – 650 °C and 4 – 700 °C temperature

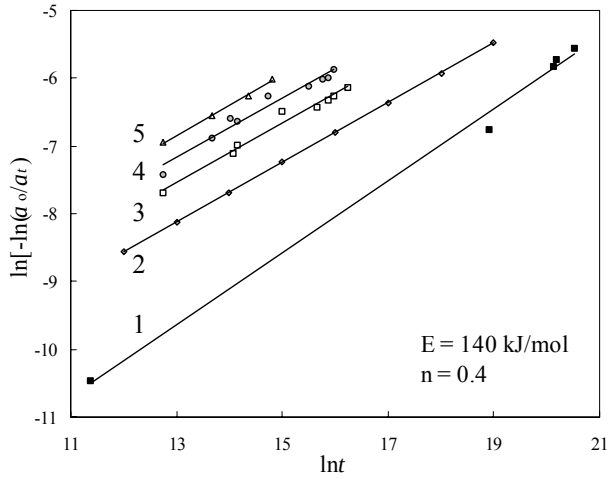

Fig. 5. The variation of $\ln[-\ln(a_0/a_t)]$ as a function of $\ln(t)$. Transformation kinetics follows the Johnson-Mehl-Avrami equation for carbide $M_{23}C_6$ in steel 12X1MΦ during its exploitation – 1, and ageing at: 3 – 600 °C, 4 – 650 °C, 5 – 700 °C. Index 2 – the evolution of calculated lattice parameter value of $M_{23}C_6$ during real exploitation

Table 2. Kinetic parameters of changes of carbide $M_{23}C_6$ cubic lattice parameter a

T, °C	$\ln k$	k
600	–30.26	$7.24 \cdot 10^{-14}$
650	–29.28	$1.93 \cdot 10^{-13}$
700	–28.23	$5.51 \cdot 10^{-13}$

$$E_a = R \cdot \frac{(\ln k_1 - \ln k_2)}{1/T_2 - 1/T_1}, \; T_1 > T_2, \tag{3}$$

which yields the value of activation energy $E_a = 140$ kJ/mol for temperature interval 600 °C – 700 °C.

The rate constant k_x, of the expected carbide $M_{23}C_6$ lattice parameter transformation in exploitation temperature, have been determined by:

$$\ln k_x = -\frac{E_a(1/T_x - 1/T_1)}{R} + \ln k_1 . \tag{4}$$

The value of $k = 2.17 \cdot 10^{-14}$ for exploitation temperature $T = 550$ °C was calculated.

The expected linear dependence of carbide $M_{23}C_6$ lattice parameter changes vs. exposition duration in the exploitation temperature (Fig. 5, curve 2) was drawn using several freely chosen duration times by equation:

$$\ln\left[-\ln\left(a_0 / a_t\right)\right] = f\left(\ln t\right), \quad (5)$$

this gives the linear dependence:

$$y = 0.44x - 113.8, \quad (6)$$

were $y = \ln[-\ln(a_0/a_t)]$ and $x = \ln t$.

The obtained expected dependence (Fig. 5, curve 2 and formula (6)) could be applied for a real temperature influence evaluation of exploited steel 12X1MΦ.

CONCLUSIONS

Although optical microscopy can reveal microstructure degradation during thermal ageing of steel but it is not exact method for actual temperature influence assessment of exploited steel 12X1MΦ state.

The X-ray diffraction qualitative phase analysis of carbides residues electrochemically extracted from steel 12X1MΦ is useful method to understand the evolution of carbide precipitation peculiarities during ageing.

The carbide $M_{23}C_6$ parameter *a* value changes from 1.05397 nm in virgin steel to 1.05698 nm aged in laboratory conditions and 1.05808 nm in steel exploited during 270000 h. Linear relationship of carbide $M_{23}C_6$ lattice parameter changes vs. service or accelerated ageing time drawn in a double logarithmic plot is particularly promising method for steel service state assessment.

REFERENCES

1. **Hahn, B., Buhl, G., Nerger, D.** In-service Condition Monitoring of Piping Systems in Power Plant Requirements and Advanced Techniques *OMMI* 1 (1) 2002: pp. 1 – 13.
2. **Laguarda, J. J., Carril, J. C., Fernandes, A. R., Valero, R. R.** Aspects of Remnant Life Assessment in Old Steam Turbines *Journal of Maritime Research* 11 (3) 2005: pp. 41 – 58.
3. **Kim, C. S., Ik-Keun Park, Kyung-Young Jhang.** Nonlinear Ultrasonic Characterization of Thermal Degradation in Ferritic 2.25Cr-1Mo Steel *NDT&E International* 42 2009: pp. 204 – 209.
4. **Starke, P., Walther, F., Eifler, D.** PHYBAL – A New Method for Lifetime Prediction Based on Strain, Temperature and Electrical Measurements *International Journal of Fatigue* 28 2006: pp. 1029 – 1036.
5. **Dasa, C. R., Albert, S. K., Bhaduri, A. K., Srinivasan, G., Murty, B. S.** Effect of Prior Microstructure on Microstructure and Mechanical Properties of Modified 9Cr-1Mo Steel Weld Joints *Materials Science and Engineering A* 477 2008: pp. 185 – 192.
6. **Ray, A. K., Tiwari, Y. N., Roy, P. K., Chaudhuri, S., Bose, S. C., Ghosh, R. N., Whittenberger, J. D.** Creep Rupture Analysis and Remaining Life Assessment of 2.25Cr-1Mo Steel Tubes from a Thermal Power Plant *Materials Science and Engineering A* 454 – 455 2007: pp. 679 – 684.
7. **Ray, A. K., Diwakar, K., Prasad, B. N., Tiwary, Y. N., Gosh, R. N., Whitetenberg, J. D.** Long Term Creep-rupture Behavior of 813 K Exposed 2.25-1Mo Steel between 773 and 873 K *Materials Science and Engineering A* 454 – 455 2007: pp. 124 – 131.
8. **Masuyama, F.** Creep Rupture Life and Design Factors for High-strength Ferritic Steels *International Journal of Pressure Vessels and Piping* 84 (1 – 2) 2007: pp. 53 – 61.
9. **Satyabrata Chaudhuri.** Philosophy of Integrity Assessment of Engineering Components *Materials Science and Engineering A* 489 2008: pp. 259 – 266.
10. **Sposito, G., Ward, C., Cawley, P., Nagy, P. B., Scruby, C.** A Review of Non-destructive Techniques for the Detection of Creep Damage in Power Plant Steels *ND&E International* 43 2010: pp. 555 – 567.
11. **Zielinski, A., Dobrzanski, J., Krzton, H.** Structural Changes in Low Alloy Cast Steel Cr-Mo-V after Long Time Creep Service *Journal of Achievements in Materials and Manufacturing Engineering* 25 (1) 2007: pp. 33 – 36.
12. **Jayan, V., Khan, M. Y., Husain, M.** Coarsening of Nano Sized Carbide Particles in 2.25Cr-1Mo Power Plant Steel after Extended Service *Materials Letters* 58 2004: pp. 2569 – 2573.
13. **Baltušnikas, A., Levinskas, R., Lukošiūtė, I.** Kinetics of Carbide Formation during Ageing of Pearlitic 12X1MΦ Steel *Materials Science* (*Medžiagotyra*) 13 (4) 2007: pp. 286 – 292.
14. **Levinskas, R., Baltušnikas, A., Lukošiūtė, I.** Assessment of State of Power Plant Steel 12X1MΦ from the Structure Point of View *Proceedings of the 13th International Conference: Mechanika 2008* 2008: pp. 314 – 319.
15. **Baltušnikas, A., Levinskas, R., Lukošiūtė, I.** Analysis of Heat Resistant Steel State by Changes of Lattices Parameters of Carbide Phases *Materials Science* (*Medžiagotyra*) 14 (3) 2008: pp. 210 – 214.
16. **Dzioba, I.** Failure Assessment Analysis of Pipelines for Heat and Power Generating Plants According to the SINTAP Procedures *International Journal of Pressure Vessels and Piping* 82 2005: pp. 787 – 796
17. PDF – 2 International Centre for Diffraction Data, 12 Campus Boulevard Newtown Square, PA 19073-3273 USA.
18. **Kraus, W., Nolze, G.** Powder Cell for Windows. Version 2.4. Federal Institute for Materials Research and Testing, Berlin. http://www.ccp14.ac.uk/tutorial/powdcell/index.html, 2008-05-26.
19. **Le Bail, A., Duroy, H., Fourquet, J. L.** Ab-Initio Structure Determination of $LiSbWO_6$ by X-Ray Powder Diffraction *Materials Research Bulletin* 23 1988: pp. 447 – 452.
20. **Lopes, Elaine, CN., dos Anjos, Fernanda, S. C., Vieira, Eunice, F. S., Cestari, Antonio, R.** An Alternative Avrami Equation to Evaluate Kinetic Parameters of the Interaction of Hg (II) with Thin Chitosan Membranes *Journal of Colloid and Interface Science* 263 2003: pp. 542 – 547.
21. **Malek, J., Mitsuhashi, T.** Testing Method for the Johnson-Mehl-Avrami Equation in Kinetic Analysis of Crystallization Processes *Journal of American Ceramic Society* 83 (8) 2000: pp. 210 – 2105.
22. **Adamaszek, K., Jurasz, Z.** Comparison of Two Methods of Calculation of Activation Energy for Some Chosen Industrial Steels after its Oxidation at High-temperatures in Air *Defect and Diffusion Forum* 237 – 240 2005: pp. 979 – 984.

Presented at the National Conference "Materials Engineering'2010" (*Kaunas, Lithuania, November 19, 2010*)

DOI: 10.5755/j02.ms.26093